Radon transform was employed for estimating angle of rotated texture by Kourosh et al [12]. Image object recognition based Radon transform was proposed by Jun Zhang et al. [13], the results of this method were robust in rotation, scale and translation invariant of image object. In the context of inclined license plates, license characters were also extracted in distorted manner. Thus, a hypothesis was formed according to the rotation alignments of the plates. Therefore, various inclined templates for different kinds of angles (from $-50°$ to $+50°$) were preserved for making rotation invariant character recognition [14]. We propose a technique for orientation detection, which is based on projection features of fan-beam, and Radon transforms. Parameter optimized Gabor filters are used to extract features from the rotation invariance image.

The remainder of the paper is organized as follows: Section II emphasizes on rotation estimation and correction of the objects using single and multi point sources. Extraction and classification of rotation invariant object by using parameter optimized Gabor filter and common classifiers are discussed in section III. Experimental results of the proposed algorithm on applying to the real-time vehicles' number plate images and check images are illustrated in section IV. Concluding remarks of this paper are given in the section V.

II. ROTATION-INVARIANCE USING LINE INTEGRALS

A vector is a quantity including both magnitude and direction, such as force, velocity, displacement and acceleration. In vector algebra, two vectors A and B are equal, if two vectors have the same direction and magnitude regardless of the position of their initial points (A=B). The ordinary integrals of vectors can be defined by

$$R(u) = R_1(u)i + R_2(u)j \ , \tag{1}$$

where $R_1(u), R_2(u)$ are specified intervals and u is a single scalar variables. Eq. (2) represents an indefinite integral of R(u).

$$\int R(u)du = i\int R_1(u)du + j\int R_2(u)du \ . \tag{2}$$

Let $r(u) = x(u)i + y(u)j$ where r(u) is the position vector of (x,y) and defines a curve C joining points P_1 and P_2, where $u = u_1$ and $u = u_2$, respectively [14]. Assume that C is balanced of a finite number of curves. For each of its curve position, vector R(u) has a continuous derivative. Let $F(x,y) = F_1 i + F_2 j$ be a vector function defined for the position. It is continuous along C. Line integral of F along C from P_1 to P_2 is defined as

$$\int_{p_1}^{p_2} F \bullet dr = \int_C F \bullet dr = \int_C F_1 dx + F_2 dy \tag{3}$$

In 2D plane, a force can be defined by a vector whose magnitude is strength of the force and direction is the path in which the force is pushed. Fig. 1 shows that force is from left to right, an object moves under the control of force and its motion is represented by the vector (S). However, force is not constant one, at different points the force may peak in different directions with strength. In accordance with these basic studies, a projection of a 2D function f(x,y) is a set of line integrals, from which data can be produced by radiating from single and multiple sources. These two sources are employed to estimate the rotation angle of the objects.

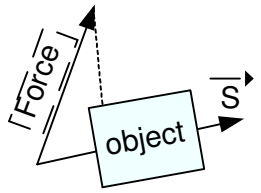

Fig. 1 Representation of force and motion in line integrals.

A 2D rotation is applied to an object by repositioning it along a circular path. A rotation angle (θ) and pivot point about which the object to be rotated are specified for generating rotation. In counterclockwise, positive angle values are used for rotation about the pivot point and in contrast clockwise rotation requires negative angle values. The rotation transformation is also described as a rotation about an axis that is perpendicular to the xy plane and passes through the pivot point. The rotation transformation equations are determined from position (x_1, y_1) to position (x_2, y_2) through an angle (B) relative to the coordinate origin. The original displacement of the point from the x-axis is (A). This is illustrated in Fig.2.

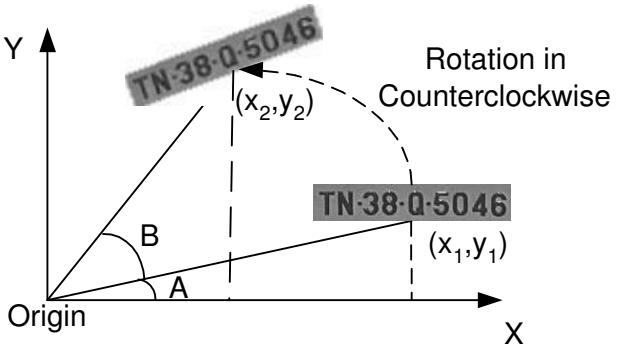

Fig. 2 Rotation of LP in counterclockwise with double angles (A, B).

The rotation can be obtained as

$$\sin(A) = y_1 / r \ ,$$
$$\sin(A+B) = y_2 / r \ ,$$

$$\cos(A+B) = x_2 / r \ \text{ and } \ \cos(A) = x_1 / r \ , \tag{4}$$

$$y_2 = x_1 \sin(B) + y_1 \cos(B) \ , \tag{5}$$

$$x_2 = x_1 \cos(B) - y_1 \sin(B) \ , \tag{6}$$

With the basics of rotation transformation and line integrals, we can introduce new ray sampling coordinates x' and y' and Jacobian (J) is described as

$$J = \left| \frac{\partial(x', y')}{\partial(x, y)} \right| = \frac{\partial x'}{\partial x} \cdot \frac{\partial y'}{\partial y} - \frac{\partial y'}{\partial y} \cdot \frac{\partial x'}{\partial y} \cdot \quad (7)$$

The fan beam projection with Radon's integral is defined as

$$f_b(r,\phi) = \frac{1}{4\pi^2} \int_{0}^{2\pi} \int_{-\infty}^{\infty} (-1/(d - r\cos(\theta - \phi))) J(x', y') dx' dy', \quad (8)$$

where $f_b(r,\phi)$ is the density at the point with polar coordinates (r,ϕ) in the region, while $(d - r\cos(\theta - \phi))$ is the perpendicular distance between the ray and this point.

A. Fan Beam Arc and Line

In this phase, projection of an image can be computed along any angle (θ). It computes the line integrals along paths that radiate from a single source. To represent an image, it performs multiple projections of the image from different angles by rotating the source around the centre of the image. Fig. 3 shows a single point source at a specified angle. This is a fan beam projection and computes the projection data as sinogram. A sinogram is an x-ray procedure that is done with contrast media to visualize any abnormal opening such as sinus in the body of the image. In the fan-beam calculation, the centre of rotation is the centre of the image and defined as

$$\lfloor size(f(x,y) + 1)/2 \rfloor, \quad (9)$$

where size(.) returns size of the rotated image f(x,y) and its lower precision value is taken for centre of rotation calculation. D is the distance in pixels from the single source point to the centre of rotation. It must be large enough to ensure that the single source point is outside the image at entire rotation angles, which is ranged from $0°$ to $359°$. The distance (D) should be larger than half the image diagonal dimension. This is described as

$$D = \sqrt{width(f(x,y))^2 + height(f(x,y))^2}\ . \quad (10)$$

After applying the fan beam projection the resultant data contains row and column of sinogram from the image f(x,y). The row data contains the number of sensor points by calculating how many beams are needed to wrap the entire image for any rotation angle. The number of column of fan data is determined by incrementing the fan rotation. It may be one degree and fan data can have 360 columns. In order to estimate the angle sensor either line-based sensor or an arc-based sensor can be used. The estimations of these two sensors are analyzed. Fan beam can be controlled by various parameters such as rotation increment, sensor geometry and sensor spacing. The rotation increment has a positive real scalar, measured in degrees, sensor geometry defines either line sensors or arc sensors and sensor spacing is used to define the spacing of the fan beam projections. If sensor geometry is 'arc' then sensor spacing has the angular spacing in degrees else linear spacing in pixel.

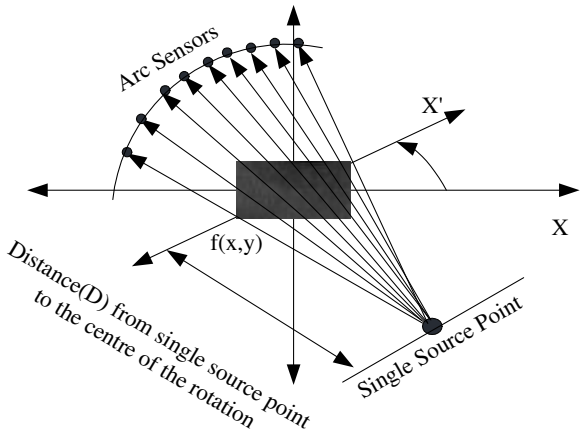

Fig. 3 Rotation estimation of segmented iris image by using arc-based sensors.

The algorithm of single source projection to estimate the angle of rotated image is as follows:

Step 1: The input image is rotated to a specific angle such as $90°$ in counterclockwise. Rotation of the image is performed using bi-cubic interpolation method.

Step 2: Specify the parameters such as distance parameter (D), rotation increment, sensor geometry and sensor spacing. In the experimentation, the rotation angles equally change from $0°$ to $359°$, D=274.8545, rotation increment = 0.1 and sensor spacing = 0.25. These values produced robust results in the estimation. The parameters of sensor geometry have not provided different estimation in all aspects. But due to sampling and numeric approximations, angle estimation may slightly be varied.

Step 3: After performing fan beam projection, fan beam projection data have been extracted from the image. In the experimentation, 92*259-size image was given and resultant fan projection data size were 1113*180. It means that fan projection provides 1113 sensors and $180°$ rotation angles. The number of sensors is determined by the fan sensor spacing. However, these size variations depend on the size of the segmented ROI of the acquired image.

Step 4: The standard deviation of fan projection data is computed to estimate the local maximum deviation of sensor data. This data set is used to calculate the maximum rotation angle of the given image that is taken as an estimated angle of the rotated image.

Step 5: The estimated angle (Φ) is used to correct the rotated image to its principal direction, which is carried out by bi-cubic interpolation method, i.e., if Φ is positive and less than $90°$ then clockwise correction is -($\Phi + 90°$) otherwise if Φ is negative and greater than $90°$ then clockwise correction is -($\Phi - 90°$).

Fig. 4 shows the step of estimation process. It illustrates the plot for estimating maximum standard deviation of 9° for the input of LP image. It also shows that prediction of angle after 90° is 99° which inferences rotation angle can also be estimated in every 90° rotation in projection of the image from single source point.

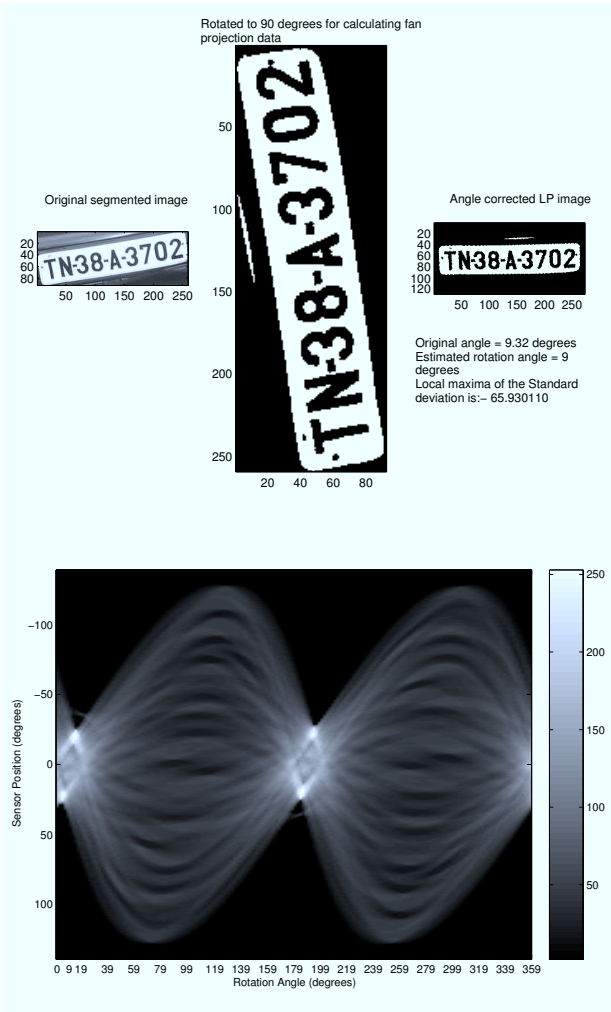

Fig. 4 Illustration of rotation correction process based on fan beam projection.

B. Estimation using Radon Transform

The basic property of Radon transform is to determine an internal constitution of an object without bodily snooping the interior structure. For this reason, It is adopted to tomography, x-ray, ultrasound, electron magnetic resonance (EMR) imaging, optics, stress analysis, geophysics and many others applications. We use multipoint sources to compute the line integrals along parallel beams in a specific direction. A projection of image f(x,y) is a set of line integrals to represent an image, this phase takes multiple parallel-beams from different angles by rotating the source around the centre of the image. This method is based on Radon transform, which estimates the angle of rotation using the projection data in different orientations. Multipoint projection computes with any angle (θ), the Radon transform of f(x,y) is the line integral of parallel paths to the y axis. The multipoint projection is defined as

$$R(x',\theta) = \int_{-\infty}^{\infty} f(x'\cos(\theta) - y'\sin(\theta), x'\sin(\theta) + y'\cos(\theta))dy', \quad (11)$$

where $R(x',\theta)$ is a Radon transform, x' is the smallest distance to the origin of the coordinate system, θ is the angle of rotation$(0-\pi)$, x' and y' are determined from the Eqs. (5-6). Radon projection data of the rotated images are used to estimate the rotation angle of the images. It uses the same algorithm of fan beam projection as given above except that it is projected angle from 0° to 179° in multi point sources. Fig. 5 depicts the process of rotation estimation of negative $(-10°)$ angle rotated image.

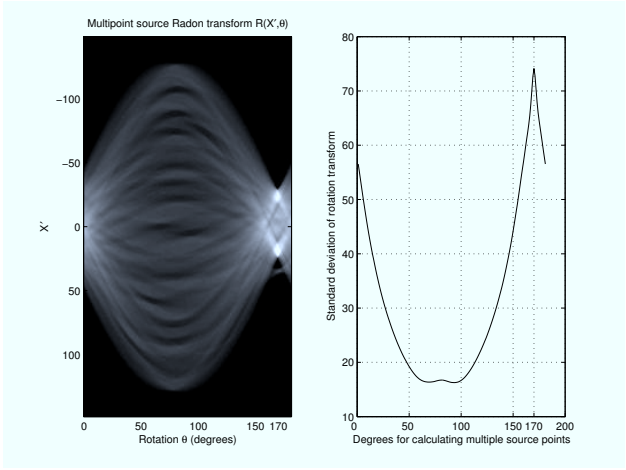

Fig. 5 Illustration of Radon multipoint source $R(x',\theta)$ and its standard deviations.

The algorithm for applying multipoint source projection to estimate the angle of rotated image is as follows:

Step 1: The given image is rotated to a specific angle such as in counterclockwise because in the real time acquisition, system can predict the initial angle of rotation. Rotation of the image is performed using bi-cubic interpolation method.

Step 2: Set the rotation angle from to and apply Eq. (11) to generate peak area of rotation angles.

Step 3: After applying the multipoint sources, for example, if the rotated image size is 99 by 277, the resultant array has 297 by 180 projection data, i.e., 297 Radon transform coefficients have been generated for each angle. The standard deviation of radon transform coefficients is calculated to find the maximum deviation of rotation angle.

Step 4: After estimating an exact angle of object rotation, it is rotated to its original principal angle by bi-cubic

interpolation method. If the estimated angle (Φ) is positive then rotate the image as -($\Phi+90°$) in clockwise direction else if the estimated angle is negative or above 90° then rotate the image as -($\Phi-90°$) in clockwise direction.

Radon projection data of the rotated images are used to estimate the rotation angle of the LP and iris images. The maximum standard deviation of Radon projection data in the range 0° to 180° from multipoint sources is 73.614521. It is treated as the maximum ($+10°$) rotation of the given image.

III. PARAMETER OPTIMIZED GABOR FILTERS

In the current literature Gabor filters and its respective feature selections have been done on a trial and error basis. These techniques are either suitable for a simple problem oriented or chosen of filter parameters in a data independent manner. Gabor filters have been calculated for feature selection in two different methods one is called filter bank and another one is filter design approach. In the former methods [15][16], parameters are chosen in an improvised manner but it did not provide optimal solution for a particular task. Another problem with these filters is the redundancy of convolutions, which demands more operations in the feature extraction. A few set of filters are designed to classify the given patterns efficiently using filter design approach which provide an optimum set of Gabor filters and reduces the computational complexity than the former one. In [17], evolutionary Gabor filter optimization method was suggested for on-road vehicle detection process. In that genetic algorithm based chromosomes were used along with incremental clustering approaches to find the optimum parameters of Gabor filters. The problem of handwritten recognition had been performed by optimized Gabor filters [18]. Those methods had used an optimum response of surface method and a puddle of predefined filters with minimum error rates operated for feature selection process. We have used the combination of Boltzmann machine with K-means clustering for choosing the best values related with frequency, orientation and scale parameters of Gabor filters. Initially, Boltzmann machine with annealing process produces optimal set of Gabor parameters. Next, K-means clustering approach is used to group the redundant response of filters generated in the optimization. Finally, according to the result of classifier design, optimum filters are collected for a particular application domain. The global optimization approach is performed to optimize the parameters of Gabor filters. The filter selection is another essential process to collect similar kind of filter parameters together, in order to collect as a single group. This is performed by taking the mean value of parameters, which provide the same type of responses. Thus, the proposed algorithm senses to remove redundant filters, reduce unnecessary convolution operations and increase the efficacy of feature extraction with a compact set of filters.

The 1-D Gabor transform was initiated by Gabor and it was extended to 2D by Daugman [19]. A 2D Gabor function is an oriented sinusoidal jarring modulated by 2D Gaussian function [22]. This is described as

$$g_{\sigma_x,\sigma_y}(x,y)=\frac{1}{2\pi\sigma_x^2\sigma_y^2}\exp\left(\frac{-1}{2}\left(\left(\frac{x}{\sigma_x}\right)^2+\left(\frac{y}{\sigma_y}\right)^2\right)\right), \quad (12)$$

$$G_{\sigma_x,\sigma_y,f,\theta(x,y)=}g_{\sigma_x,\sigma_y}(x,y).\exp(2\pi jf(x\cos\theta+y\sin\theta)), \quad (13)$$

where $g_{\sigma_x,\sigma_y}(x,y)$ is the Gaussian with scale parameter parameters (σ_x,σ_y), these parameters determine the effective size of the neighbourhood operation of a pixel in which the weight convolution is carried out, f is the centre frequency which is a span-limited sinusoidal grating. θ specifies the orientation of the normal to the parallel stripes of a Gabor function. Its value is specified in degrees ranging from $0°$ to $360°$. However, θ is considered in between 0 degrees and 180 degrees because symmetry makes the other orientation redundant. In the specific application orientation θ can be computed as $\theta_o=\pi(o-1)/n$, $o=1,2,3...n$ where π radians = 180 degrees, 1 radian = $(180°/\pi)$ and n represents number of orientations maintained in the system. The Gabor filter $G_{\sigma_x,\sigma_y,f,\theta(x,y)}$ forms complex valued function and it is composed into real and imaginary parts as

$$G_{\sigma_x\sigma_y,f,\theta}(x,y)=R_{\sigma_x\sigma_y,f,\theta}(x,y)+jI_{\sigma_x\sigma_y,f,\theta}(x,y), \quad (14)$$

$$\begin{aligned}R_{\sigma_x,\sigma_y,f,\theta}(x,y)&=g_{\sigma_x\sigma_y(x,y)}\bullet\cos[2\pi f(x\cos\theta+y\sin\theta)],\\ I_{\sigma_x,\sigma_y,f,\theta}(x,y)&=g_{\sigma_x\sigma_y(x,y)}\bullet\sin[2\pi f(x\cos\theta+y\sin\theta)]\end{aligned} \quad (15)$$

A. Parameter Selection and Conditions

In this phase, parameter selection for Gabor filters is discussed. It determines the best way to find the parameters set for the given problem domain. A best parameter set $G_P=\{\theta,f,\sigma_x,\sigma_y\}$ is determined by the proposed approach. Initially, the parameters should satisfy the Eq. (16).

$$0°\le\theta\le180, f_{\min}\le f\le f_{\max,}\sigma_{\min x}\le\sigma_x\le\sigma_{\max x},\sigma_{\min y}\le\sigma_y\le\sigma_{\max y}, \quad (16)$$

where $\theta_o=\pi(o-1)/n, o=1,2,...,n,$ $f_{\min},f_{\max}$ denote minimum and maximum frequency wave length assigned by the system, $\sigma_{\min x},\sigma_{\max x}$ represent minimum and maximum standard deviation of Gaussian envelope which is used for assigning scale parameters, $\sigma_{\min y},\sigma_{\max y}$ signify minimum and maximum of y-direction scale factor.

The four parameters $P=\{\theta,f,\sigma_x,\sigma_y\}$ are selected for determining each Gabor filter. Thus, selecting a set of Gabor filter for a problem specific domain is related with optimizing these four parameters efficiently. Perhaps, a pattern recognition application needs G filters then 4*G parameters involve to be optimized. For example, if 20 filters are required by the application then 80 parameters are to be optimized. In general, optimizing such a large dimensional problem is more difficult and consequently it demands more time complexity to achieve the optimal states. The Boltzmann optimization method is used

for optimizing the parameter space of the Gabor filters. This network accepts bipolar features as set of input units and the output units represent the output categories. It is nothing but a recurrent network consisting of N two state units. These states can be chosen from bipolar space, that is, each Gabor filter parameters are converted to bipolar string as it looks like $P = \{1,-1\}^N$. If G filters are necessary for the filter design and parameters required M bipolar string then G*M length of patterns are needed. Each of the four parameters in P is a determined using M/4 bipolar pattern. The energy function of the Boltzmann machine is defined as

$$E(P) = -1/2 \sum_{i,j=1}^{N} w_{ij} p_i p_j \,, \tag{17}$$

where the w_{ij} is set of weight vector, and can be either positive or negative, $w_{ii} = 0$ is a prerequisite for converging the network. The main objective of Boltzmann machine is to reach the global minimum of its energy function, which is the minimum energy of the state. Thus it uses a stochastic acceptance criterion, thus allowing it to escape from its local minima. Let P denote the state space of the machine that is the set of all possible states. Among these, the state vectors differing by one bit are called neighbouring states. The neighborhood $N_p \subset P$ is defined as the set of all neighboring states of p. Let p^j, the neighboring state obtained from p by changing the state of neuron j be defined as

$$P_i{}^j = \begin{cases} +\, p_i & if \quad i \neq j \\ -\, p_i & if \quad i = j \end{cases} \qquad P \in (1,-1)^N,\ P^j \in N_p \,, \tag{18}$$

The difference in energy when the global state of the machine is changed from P to p^j is denoted as

$$\Delta E(p^j \mid p) = E(p^j) - E(p). \tag{19}$$

Note that the contribution of the connections $W_{km}, k \neq j, m \neq j$ to E(P) and $E(P^j)$ is identical if $W_{ij} = W_{ij}$, this described as

$$\Delta E(P^j \mid P) = (2P_j)(\sum_{i}^{N} W_{ij} P_i) \quad P \in (1,-1)^N, W_{ii} = 0. \tag{20}$$

Therefore, the change in the energy can be computed by considering only local information. The Boltzmann machine can escape from the local minima because of its probabilistic nature. Two phases involve in the optimization using Boltzmann machine, in the first phase, an energy function for the given application is decided. In the constrained optimization, the energy function must be derived using both the original cost function and constrains. In contrast, the energy function can be directly obtained by using the cost function in the non-constrained applications. Next in the second phase, machine searches global minimum through the annealing procedure. The algorithm runs for a certain number of iterations controlled by the temperature and in each state try to find equilibrium. The temperature is reduced or increased in a controlled manner by the parameters α^A or β^A, respectively. The annealing is terminated when the time exceeds the permitted time.

K-means partitions the observations of optimized Gabor parameters into k mutually exclusive clusters and returns a vector of indices indicating to which of the k clusters it has assigned each observation. K-means is more suitable for clustering large amounts of data because it groups the Gabor parameters using their local-maximum-likelihood estimations. It takes each observation of parameter data as an object having a location in space and seeks a partition in which objects within each cluster are as close to each other cluster as feasible, and as far away from objects in other clusters as feasible. If the application needs twelve diverse distance measures then depending on the kind of optimized parameters the cluster can be grouped. The algorithm of K-means clustering as follows:

Step 1: Assign the number of optimized Gabor filters parameters that are provided indistinguishable responses.

Step 2: Initialize the number of clusters needed for the application domain. That is, according to these parameters such as orientation, frequency, scaling factor of x and y directions the cluster can be formed.

Step 3: Compute $\hat{\mu}_i = \frac{\sum_{k=1}^{n} \hat{P}(\omega_i \mid x_k, \hat{\theta}) x_k}{\sum_{k=1}^{n} \hat{P}(\omega_i \mid x_k, \hat{\theta})}$ for K different clusters.

Step 4: Classify the number of optimized Gabor parameters according to the nearest $\hat{\mu}_i$

Step 5: Compute the next mean vector $\hat{\mu}_{i+1}$ for the same cluster.

Step 6: Repeat the step 4 and step 5 until $|\hat{\mu}_i - \hat{\mu}_{i+1}|$ = Threshold.

Step 7: Compute the mean vector for the remaining number of clusters. Finally, groups of K divergent clusters are formed. From these clusters the mean values of single filter parameters are chosen as a Gabor filter. Thus K numbers of Gabor filters are selected for the convolution process.

However, Gabor filter produces local band pass frequency for rotation-invariant recognition. Its accuracy is limited to local orientation of shifting of pixels alone. In large extent orientations, Gabor filter produces more false positives for intra-class. Therefore, we overcome the problem of making features as rotation invariant by estimating and correcting orientations before applying rotation invariant Gabor filters. Hence, it provides a complete set of features, which are invariant to large variations of orientations in real-time acquisitions. In addition, it assists the classifiers not to settle in converging state of local orientation features for intra-classes patterns and tends to get global rotation-invariants [23].

IV. PERFORMANCE ANALYSIS AND EXPERIMENTS

In order to evaluate the efficacy of the estimation process, comparison of rotation estimation of projection data of fan beam arc, fan beam line and Radon transform have been carried out. These methods respond a bit different response of peak projection data at a particular angle. These variations occur due to high frequency of the components present in the images. Among these methods Radon and fan beam line provide narrow peak estimation than the fan arc method because it produces little bit wide angle in all the angles like 0, 45 and 90 degrees as shown in Fig 6. However, due to illumination changes in twilight and nighttime, LP image rotation estimation is crucial factor and its illumination level should be estimated before estimating the rotation angle for binarization. After rotation correction, optimized Gabor filters are applied to extract rotation-invariant features, which give more accuracy than the traditional Gabor filters because, the optimized approach searches filter parameters which are provided high separability in the classification. Moreover, before feature extraction, real-time images' orientation are corrected its principal direction that afford more positive intra-class classifications. Thus incorporation of optimizing Gabor filters with real-time orientation correction produces higher interclass separability than other existing approach.

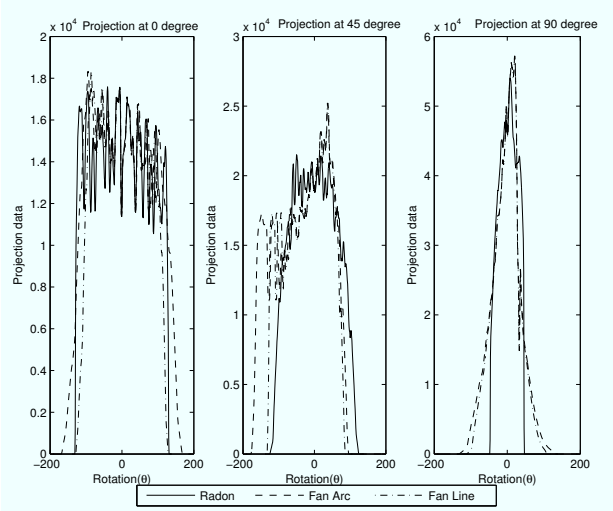

Fig. 6 Comparison of projection data in the particular angles.

Two phases of experiments were conducted for evaluating the efficacy of the proposed system. In the first phase, image orientation estimation was analyzed and results are studied. Classification rate of the rotation-invariant features based on classifiers were studied in the second phase. Our database has 535 images, which are acquired in different illuminations. It consists of 237 license plates and 298 eye images. In the real-time, license plate images were captured in 45 different angles of rotation varying from 4° onwards. 9 different angles of iris images were captured by changing its orientation. Experimental results reveal that fan-arc (FA) method causes more errors in the estimation process than the rest of the methods such as fan-line (FL) and Radon transform (RD). This was mainly due to approximation of numeric value of projection data and selection of sensor sources. However, these errors may not produce more false positives in the recognition process because error differences are very smaller than the actual capturing orientations. Furthermore, vehicle images are also captured from $-1°$ to $-90°$ in clockwise directions to test the estimation algorithm. In addition to that, acquired images are added Gaussian noise with local variance to check the efficiency of the proposed method. The average estimation of rotation angle variation was slightly diverged between noise and clear images. However, estimation angle was not widely varied for noisy images. Fig 7 shows the result of projection data of these methods at 0, 45 and 90 degrees.

Due to factor of high gray level magnitude in iris patterns all the three estimation methods have produced the slight variation in the estimation process.

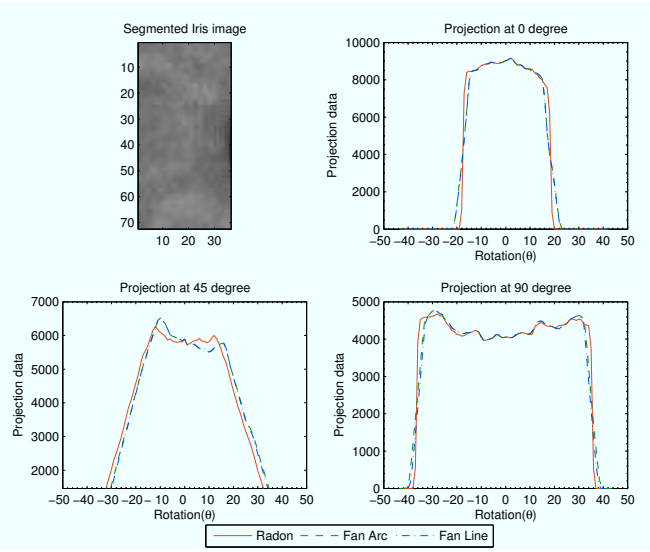

Fig. 7 Iris image orientation estimation with FA, FL and RD methods.

The rotation estimation of license plate images is also carried out with FA and FL and RD methods. These methods respond a bit different from peak projection data at a particular angle. These variations occur due to high frequency of the components present in the LP images. Among these methods Radon and fan beam line provide narrow peak estimation than the fan arc method because it produces little bit wide angle in all the angles like 0, 45 and 90 degrees as shown in Fig 8. However, due to illumination changes in twilight and nighttime, LP image rotation estimation is a crucial factor and its illumination level should be estimated before estimating the rotation angle for binarization.

In order to evaluate the robustness of the method, Zero-mean Gaussian white noise with an intensity dependent variance and Poisson noises are added to the segmented image. After estimating the expected rotation angle of the image, it can be skewed to its principal angle using bi-cubic interpolation method. These algorithms are tested with diverse eye images in real time conditions. In the capturing process, subjects' head

moments are directed to acquire the eye images by different rotation angles.

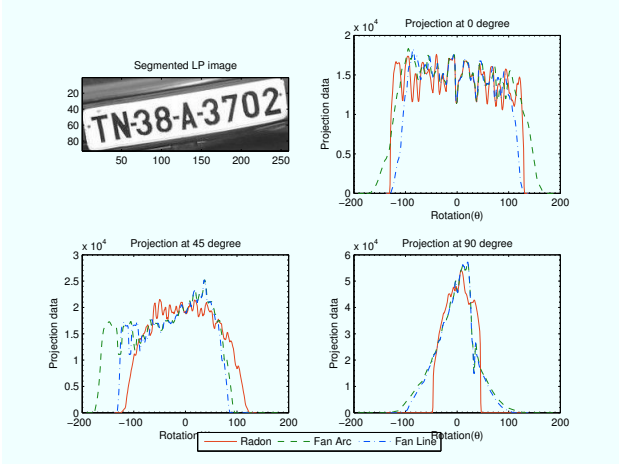

Fig. 8 License plate image orientation estimation with FA, FL and RD methods.

Hence, eye images were captured in 0° to 90° in both clock and anticlockwise directions. However, as far as iris recognition is concerned, head moments are in left, right, bottom and top directions only. Thus, the maximum rotation of angles was from 0° to 45° for the estimation process. Moreover, in the experimentation Gaussian white noise, Poisson noises and eye wears noises were added up to verify the robustness of the proposed approaches. Fig. 9 shows the rotation estimation with noisy iris patterns.

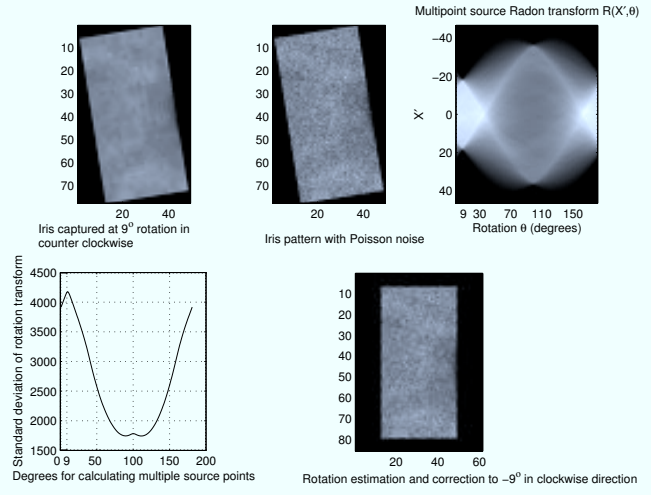

Fig. 9 Rotation estimation in noisy iris images.

After generating Poisson noises, iris pattern's pixel intensity is altered based on the number of photons of pixel information and the mean square signal-to-noise ratio (SNR) of the resultant image which was 31.6048. However, noisy data occur in the iris pattern that may not affect the estimation process because projection data of the estimation process were approximately equivalent to the clear images, i.e., it was produced as maximum of standard deviation magnitude. Hence, noisy iris pattern acquired due to eyewear and environment illuminations may slightly affect the estimation process. The result comparison of these methods has been shown in Table I.

TABLE I. RESULTS OF IRIS IMAGES ROTATION ESTIMATION

Actual orientation in degree	No. of sample rotated images	Rotation Estimation in degree			Average Rotation correction in degree			Average error rate in degree		
		FA	FL	RD	FA	FL	RD	FA	FL	RD
3	47	3.4	3.3	3.2	3.3	3.3	3.2	0.3	0.3	0.2
9	56	9.5	9.4	9.4	9.5	9.4	9.4	0.5	0.4	0.4
15	68	15.7	15.4	15.3	15.6	15.5	15.4	0.6	0.5	0.4
20	40	20.8	20.6	20.5	20.7	20.6	20.5	0.7	0.6	0.5
30	72	31	30.7	30.8	31	30.8	30.8	1	0.8	0.8
45	64	46.6	46	46	46.5	46	46	1.5	1	1
-5	42	-4.5	-4.6	-4.8	-4.4	-4.6	-4.7	-0.6	-0.4	-0.3
-15	32	14.3 (-)	14.5 (-)	14.8 (-)	14.3 (-)	14.4 (-)	14.7 (-)	-0.7	-0.6	-0.3
-20	46	19.1 (-)	19.4 (-)	19.5 (-)	19 (-)	19.5 (-)	19.5 (-)	-1	-0.5	-0.5

TABLE II. INCORPORATION OF NOISY MEASURE IN ROTATION ESTIMATION OF IRIS IMAGES

Noise type	Mean square	Error Square	SNR_{ms}	Root Mean square error
Poisson	606198	23036	26.315246	2.470928
Zero-mean Gaussian	564368	194464	2.902172	7.179203
Gaussian Mean=0,variance=0.01	605038	75772	7.984981	4.481372
Eye wears	261258	62934	4.151301	4.927483

From further investigation, we can understand that in worst-case rotation estimation the average error rate between actual orientation and correction angles were reported by FA method. It produced 1.5-degree error, while estimating 45-degree iris rotation patterns, whereas RD and FL produced better result than FA and it's worst-case estimation error is reported 1°. This is shown in Fig 10. However, the minimum errors in rotation estimation may not affect the recognition process. It outperforms the other methods as maintained by the template matching of iris patterns in different angles and a bit shifting in left or right while matching the iris patterns. Hence this method removes the overburden of storing additional iris patterns for compensating rotation invariants and it eliminates shifting of iris bits in the recognition. Thus computational complexity is considerably reduced by the proposed approach. Table II shows the noise measures incorporated in the iris rotation estimation process.

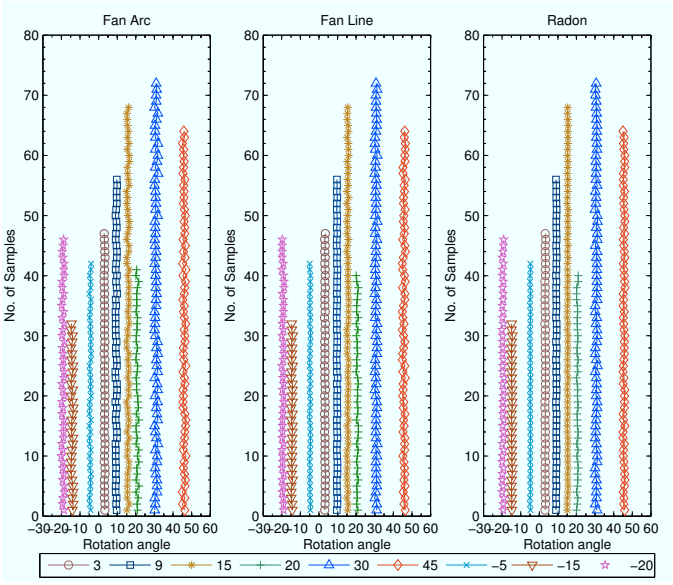

Fig. 10 Estimation result of rotation estimation of real-time iris images.

In order to evaluate parameter optimized Gabor features we have conducted experiments with different measures of classifiers. In the recognition phase, correct accept rate (CAR) and false positive rate (FAR) of the training sets were evaluated for the different classifiers. Training set consists of 142 and 154 samples of license plates and iris images, respectively. The reminder samples were treated as test samples. The CAR of the diverse classifiers was observed, it was: Hamming neural network 98.37%, back propagation network 97.02%, Euclidean-norm distance 94.86% and k-nearest neighbor-94.32%. Fig.11 shows receiver operating characteristics curve (ROC) of the recognition process of different classifies using parameter optimized Gabor features.

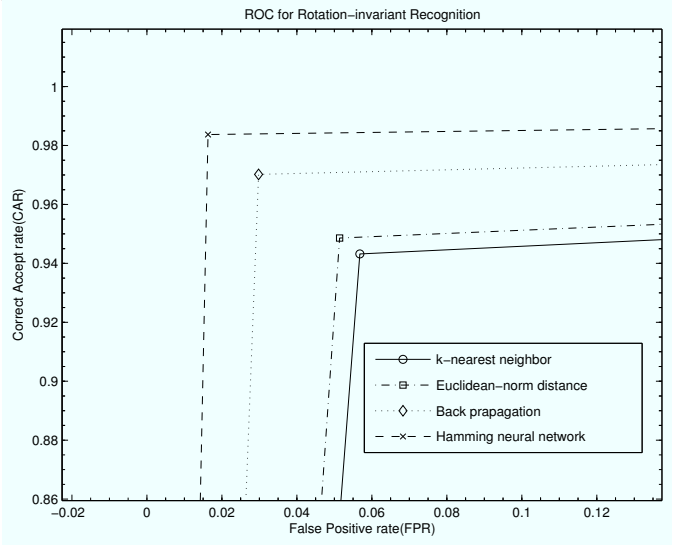

Fig. 11. ROC of Rotation invariant recognition with diverse classifiers.

V. Conclusion

In view of the fact that there is no an appropriate set of signal present in the image, it is a difficult process to estimate its orientation while capturing image at diverse angles. In this paper, we proposed a method which is based on line integrals. It projected the captured data using fan-arc, fan-line and Radon transform methods to estimate the maximum angle variations. The suggested algorithms will be further extended to estimate the orientation angle of face, fingerprints, palm, electron magnetic resonance and other kind of images with minimum estimation error. In the context of invariant recognition, the estimation process is possibly incorporate with parameter optimized Gabor filter. It achieved the sufficient rotation invariance of features and produced better accuracy for the real-time patterns with a compact set of characteristics. This paper opens a new direction of research in the computer vision committee to acknowledge the rotation estimation and invariant problems with relative simplicity, accuracy and robust to noise.

Acknowledgment

Authors thank their family members and children for their continuous support and consent encouragement to do this research work successfully.

References

[1] R.Bremananth, A.Chitra, Vivek seetharaman, Vidyasudhan, A new methodology for License plate recognition system, *IETE Journal of Research*, 51(4), 2005, 279-286.

[2] Park S.H, Kim K.I, Jung K and Kim H.J, Locating Car License Plate using Neural Networks, *IEE Electronics letters, 35(17)*, 1999,1475–1477.

[3] Takashi Naito, Toshihiko Tsukada, Keiichi Yamada, Kazuhiro Kozuka, and Shin Yamamoto, Robust License-Plate Recognition Method for Passing Vehicles Under Outside Environment *IEEE Transactions on Vehicular Technology, 49(6)*, 2000, 2309–2319.

[4] Bonnet S, Peyrin F, Turjman F and Prost R, Multiresolution reconstruction in Fan-beam Tomography, *Proc. of IEEE Nuclear Science Symposium Conference*, 2, 2000, 15/105-15/109.

[5] Ojala T, PietikainenM and Maenppa T, Multiresolution gray-scale and rotation invariant texture classification with local binary patterns, *IEEE Transactions Pattern Analysis and Machine Intelligence, 24(7)*, 2002,.971-987.

[6] Pietikainen M, Ojala T and Xu Z, Rotation-invariant texture classification using feature distributions, *Pattern Recognition, 33*, 2000, 43-52.

[7] Mao J and Jain A.K, Texture classification and segmentation using multiresolution simultaneous autoregressive models, *Pattern recognition, 25 (4)*, 1992,173-188.

[8] Aditya Vailaya, Hong Jiang Zhang, Changjiang Yang, Feng-I Liu and Anil K. Jain, Automatic Image Orientation Detection, *IEEE Transactions on Image Processing, 11(7)*, 2002, 746-755.

[9] Chen J.L and Kundu A.A ,Rotation and Gray scale transformation Invariant Texture Identification Using Wavelet Decomposition and Hidden Markov Model, *IEEE Transactions on pattern analysis and Machine Intelligence, 16(2)*, 1994,208-214.

[10] Lian cai and Sidan Du, Rotation, scale and translation invariant image watermarking using Radon transform and Fourier transform, *Proc. of the IEEE 6th Circuit and systems Symposium Emerging Technologies: Mobile and Wireless Communication*, 2004, 281-284.

[11] Mitra Abhishek and Banerjee S, A Regular Algorithm For Real Time Radon and Inverse Radon Transform, *Proc. of IEEE Acoustics, Speech and Signal Processing (ICASSP)*, 2004,105-108.

[12] Kourosh Jafari-Kkouzani and Hamid Soltaian-Zadeh, Rotation-Invariant Multiresolution Texture analysis using Radon and Wavelet Transforms, *IEEE Transactions on Image processing, 14(6)*, 2005, 783-795.

[13] Jun Zhang, Xiyuan Zhou and Erke Mao, Image Object Recognition based on Radon Transform, *Proc. of IEEE 5th World Congress on Intelligent Control and Automation*, 2004, 4070-4074(0-7803-8273-0/04).

[14] Murray R Spiegel, Theory and problems of Vector analysis, (SI (metric)Edition,Schaum's outline series, Singapore, 1974 (ISBN:0-07-099009-3)).

[15] Anil K. Jain, S.Prabhkar, L. Hong and S.Pankathi, Filter-Bank Based Fingerprint Matching, *IEEE Trans. on Image Processing, 9(5)*, 2000, 846-859.

[16] Namuduri K. R, R. Mehrotra and N. Ranganathan, Efficient computation of Gabor filter based multiresolution responses, *Pattern Recognition 27*, 1994 925-938.

[17] Zehang Sun, George Bebis, and Ronald Miller, On-Road Vehicle Detection Using Evolutionary Gabor Filter Optimization, *IEEE Transactions on Intelligent Transportation Systems, 6(2)*, 2005, 125-137.

[18] HamamotoY., Uchimura S., Watanabe M, Yasuda T, Mitani Y and Tomota S., A Gabor Filters-based Method For Recognizing Handwritten Numerals, *Pattern recognition, 31(4)*, 1998, 395-400.

[19] Daugman John G , Complete Discrete 2-D Gabor Transforms by Neural Networks for Image Analysis and Compression, *IEEE Transactions on Acoustics, Speech, and signal processing, 36(7)*, 1988,1169-1179.

[20] R. Bremananth, Prof. A. Chitra, 'A new approach for iris pattern analysis based on wavelet and HNN', Journal of the Computer Society of India, Vol.36, No.2, pp.33-41, 2006.

[21] R. Bremananth, Prof. A. Chitra, 'Real-Time Image Orientation Detection and Recognition', International Conference on Signal and Image Processing (ICSIP), Dec. 2006, pp.460-461.

[22] Bremananth R. and Chitra A 'Rotation Invariant Recognition of Iris', Journal of Systems Science and Engineering, Systems Society of India, Vol.17, No.1, pp.69-78, 2008.

[23] Bremananth R, Ph.D. Dissertation, Anna University, Chennai, India, 2008.

AUTHORS PROFILE

Bremananth R received the B.Sc and M.Sc. degrees in Computer Science from Madurai Kamaraj and Bharathidsan University, respectively. He obtained M.Phil. degree in Computer Science and Engineering from GCT, Bharathiar University. He received his Ph.D. degree in 2008 from Department of Computer Science and Engineering, PSG College of Technology, Anna University, Chennai, India. He has 16+ years of experience in teaching, research and software development at various Institutions in India. Presently, he is working as a Research Fellow, at Nanyang Technological University, Singapore. He received the M N Saha Memorial award for the best application oriented paper in 2006 by Institute of Electronics and Telecommunication Engineers (IETE). His fields of research are acoustic holography, pattern recognition, computer vision, image processing, biometrics, multimedia and soft computing. Dr. Bremananth is a member of Indian society of technical education(ISTE), advanced computing society(ACS), International Association of Computer Science and Information Technology(IACIT) and IETE.

Andy W. H. Khong received the B.Eng. degree from Nanyang Technological University, Singapore, in 2002 and the Ph.D. degree from Department of Electrical and Electronic Engineering, Imperial College London, London, U.K., in 2005. He is currently an Assistant Professor in the School of Electrical and Electronic Engineering, Nanyang Technological University, Singapore. Prior to that, he was a Research Associate (2005-2008) in the Department of Electrical and Electronic Engineering, Imperial College London. His postdoctoral research involved in developing signal processing algorithms for vehicle destination inference as well as the design and implementation of acoustic array and seismic fusion algorithms for perimeter security systems. He was the recipient of the best student paper award at the International Workshop on Acoustic Echo and Noise Control 2005. His Ph.D.research was mainly on partial-update and selective-tap adaptive algorithms with applications to mono- and multichannel acoustic echo cancelation for hands-free telephony. He has also published works on acoustic blind channel identification for speech dereverberation. His other research interests include speech enhancement and blind deconvolution algorithms. Dr. Andy is a life member of IEEE.

Mrs. M. Sankari received her B.Sc. and M.Sc. degrees in Computer science from Bharathidasan University, respectively. She has completed her Master of Philosophy degree in Computer science from Regional Engineering College, Trichy. Presently, she is a Head of the department of Computer Application department at NIET and pursuing her doctorate degree in Computer science at Avinashilingam University, Coimbatore, India. She has published various technical papers at IEEE conferences. Her field of research includes Computer vision, Pattern recognition, Analysis of algorithms, Data structure, Computer graphics and multimedia.